computation

MDPI

Article

Plasma Confined Ground and Excited State Helium Atom: A Comparison Theorem Study Using Variational Monte Carlo and Lagrange Mesh Method

Salah B. Doma [1], Mahmoud A. Salem [2] and Kalidas D. Sen [3,*]

[1] Faculty of Science, Alexandria University, Alexandria 21544, Egypt; sbdoma@alexu.edu.eg
[2] Department of Basic and Applied Sciences, Arab Academy for Science, Technology and Maritime Transport, Alexandria 21544, Egypt; mahmoud_ms2008@yahoo.com
[3] School of Chemistry, University of Hyderabad, Hyderabad 500046, India
* Correspondence: kds77@uohyd.ac.in

Abstract: The energy eigenvalues of the ground state helium atom and lowest two excited states corresponding to the configurations 1s2s embedded in the plasma environment using Hulthén, Debye–Hückel and exponential cosine screened Coulomb model potentials are investigated within the variational Monte Carlo method, starting with the ultracompact trial wave functions in the form of generalized Hylleraas–Kinoshita functions and Guevara–Harris–Turbiner functions. The Lagrange mesh method calculations of energy are reported for the He atom in the ground and excited ^1S and ^3S states, which are in excellent agreement with the variational Monte Carlo results. Interesting relative ordering of eigenvalues are reported corresponding to the different screened Coulomb potentials in the He ground and excited electronic states, which are rationalized in terms of the comparison theorem of quantum mechanics.

Keywords: helium atom; screened Coulomb potential; variational Monte Carlo method; Lagrange mesh method; comparison theorem

Citation: Doma, S.B.; Salem, M.A.; Sen, K.D. Plasma Confined Ground and Excited State Helium Atom: A Comparison Theorem Study Using Variational Monte Carlo and Lagrange Mesh Method. *Computation* **2021**, *9*, 138. https://doi.org/10.3390/computation9120138

Academic Editor: Henry Chermette

Received: 23 November 2021
Accepted: 7 December 2021
Published: 10 December 2021

1. Introduction

The theoretical studies of atomic systems in dense plasmas at different temperatures play a very important role in some physical situations and have gained considerable interest in recent years [1–8]. The dilute plasma environment is represented by the screened Coulomb potentials given by the Debye–Hückel model (DHM) or screened Coulomb potential (SCP) [9], which provides a suitable treatment of nonideality in plasma via the screening effect under the low-density and high-temperature conditions. A closely related Hulthén potential is also used as a model potential for the dilute plasma environment in which the atoms are embedded. On the other hand, the dense quantum plasmas environment is represented by using the modified Debye–Hückel model (MDHM) [10] or exponential cosine screened Coulomb potential (ECSCP). Due to its oscillatory nature, the MDHM potential represents a stronger screening effect than the DHM potential.

Considerable attention has been given to the screened Coulomb potentials and exponential cosine screened Coulomb potential in field theory, nuclear, and plasma physics [11–17]. Accurate B-spline configuration interaction (BSCI) method was recently employed to study the spectral/structural data of the helium atom with exponential cosine screened Coulomb potentials [18]. Roy [19] discussed the critical parameter for the spherically confined H atom embedded within a diverse set of screened Coulomb potentials. Ghoshal and Ho [20] investigated the two-electron system in the field of generalized screened potential within the framework of highly correlated and extensive wave functions in Ritz's variational principle, where they were able to determine accurate ground state energies and wave functions of the two-electron system for different values of the screening parameter. Nasser, Zeama, and

Abdel-Hady [21] made a comparative study of the atomic Rényi and Shannon entropies with different wave function within the ECSCP for the $1s^2$-state of the helium isoelectronic series in the Hylleraas-space with few variational parameters. Several other interesting studies on the few electron atoms embedded inside the different plasma potentials have been presented in the literature [22–24]. Very recently a comprehensive compilation of accurate energy values and other structural parameters for the He-like atoms has been published [25,26] using the Hylleraas wave functions.

The purpose of this paper is twofold. Firstly, we report the energy values corresponding to the ground state and two low-lying excited electronic states of the He-like atoms embedded in three different plasma environments using the variational Monte Carlo (VMC) method [27–31] and the Lagrange mesh method (LMM) [32]. The second purpose of this work concerns with the application of the comparison theorem of quantum mechanics. According to the comparison theorem, if a set of spherical potentials $V_1(r)$, $V_2(r)$, $V_3(r)$ satisfy the condition $V_1(r) < V_2(r) < V_3(r)$ at all radial distances, then their eigenvalues obey $E_1 < E_2 < E_3$ for all $n\ell$-states. For nonrelativistic Hamiltonians bounded from below, this theorem follows directly from the variational characterization of the eigenspectrum [33]. Generalized comparison theorems have been proposed [34–38] that allow the two potential curves to cross over in a controlled fashion while maintaining a definite ordering of the respective eigenvalues. Refined comparison theorems applicable to the relativistic Dirac Hamiltonian, which is not bounded from below, have also been established [39–41]. We refer to the works on the generalized comparison theorem [42] and the refined comparison theorem [43], which covers the current research trends in this area. In this work, we used the comparison theorem in order to rationalize the relative ordering of eigenspectra of the He atom under a set of different plasma screened Coulomb potentials for the ground and a few low-lying excited states. To the best of our knowledge, a comprehensive numerical test of the comparison theorem using the VMC and the LMM computations including the excited states, as reported in this work, has not been attempted earlier.

The outline of this paper follows. In Section 2, we define the three different screened Coulomb model potentials that are introduced above. In Section 3, an outline of the variational Monte Carlo (VMC) method employed in this work is presented. This is followed by the computational details and the choice of the trial wave functions for the low-lying excited states of He, described in Sections 4 and 5, respectively. A brief description of the Lagrange mesh method employed in this work is presented in Section 6. Our results are presented and discussed in Section 7. Finally, the main conclusions of this work are listed in Section 8.

2. Plasma Model Potentials

The collective effects of correlated many-particle interactions lead to screened Coulomb interactions in hot dense plasma conditions, which are commonly represented by the DHM or SCP and given by

$$V_{DH}(r) = -\frac{Ze^2}{r} exp(-\mu r), \tag{1}$$

where $\mu = \frac{1}{\lambda_D}$ represents the Debye screening parameter that determines the electronic interaction in the Debye plasma. It depends on the temperature and density of the plasma in the following form [44]:

$$\mu = \frac{1}{\lambda_D} = \sqrt{4\pi e^2 N_e / KT_e}, \tag{2}$$

where λ_D is called Debye screening length, K is the Boltzmann constant, T_e is the electron temperature, e is the electronic charge, Z is the atomic number, and N_e is the plasma–electron density. The Hulthén [45] potential is given by

$$V_{Hu\_\mu}(r) = -Ze^2 \frac{\mu e^{-\mu r}}{1 - e^{-\mu r}}\,. \tag{3}$$

A useful form of Hulthén potential in which the screening parameter μ in Equation (3) is simply multiplied by a factor of 2 can be defined as

$$V_{Hu\_2\mu}(r) = -Ze^2 \frac{2\mu e^{-2\mu r}}{1 - e^{-2\mu r}}. \tag{4}$$

It was shown that the study of effective screened potential in dense quantum plasmas can be represented by using MDHM [10] or ECSCP, which is given by

$$V_{MDH}(r) = -\frac{Ze^2}{r} exp(-\mu r)\cos(\mu r). \tag{5}$$

Usually, in quantum plasmas, μ is related to the quantum wave number of the electron, which is related to the electron plasma frequency. Furthermore, the definitions of μ in the two model potentials are different. In the present paper, we are considering μ as a parameter so that the physical difference of μ between these model potentials [14,19,46] is not discussed.

3. Variational Monte Carlo Method

Quantum Monte Carlo methods have already been used for quantum mechanical systems. There are several quantum Monte Carlo techniques such as VMC, diffusion Monte Carlo and Green's function Monte Carlo methods. In this paper, we concentrate on the VMC method, which is used to approximate the eigenstate of the Hamiltonian $\hat{H}$ of a quantum mechanical system by some trial wave function $\psi_T(R)$ whose form is chosen from the analysis of the quantum mechanical system under study. Therefore, the expectation value of the Hamiltonian $\hat{H}$ is written as [46]

$$\hat{H} = E_{VMC} = \frac{\int \psi_T^*(R)\hat{H}\psi_T(R)dR}{\int \psi_T^*(R)\psi_T(R)dR} = \frac{\int dR\psi_T^2(R)E_L(R)}{\int dR\psi_T^2(R)} = \int dR\, \rho(R)E_L(R) \tag{6}$$

where $E_L(R) = (H\psi_T(R))/\psi_T(R)$ is the local energy depending on the $3N$ coordinates R of the N electrons, and $\rho(R) = \frac{\psi_T^2(R)}{\int dR\psi_T^2(R)}$ is the normalized probability density. The variational energy can be calculated as the average value of $E_L(R)$ on a sample of M points R_k, sampled from the probability density $\rho(R)$ as follows:

$$E_{VMC} \approx E_L = \frac{1}{M}\sum_{k=1}^{M} E_L(R_k). \tag{7}$$

In practice, the points R_k are sampled using the Metropolis–Hastings algorithm [27,28].

When evaluating the energy of the system it is important to calculate the standard deviation of this energy, given by [47]

$$\sigma = \sqrt{\frac{\langle E_L^2\rangle - \langle E_L\rangle^2}{N(M-1)}}.$$

Since E_L will be exact when an exact trial wave function is used, then the standard deviation of the local energy will be zero for this case. Thus, in the Monte Carlo method, the minimum of E_L should coincide with a minimum in the standard deviation.

4. Theoretical Details

The nonrelativistic Hamiltonian in Hylleraas coordinates [47] for the two electron systems, under effective SCP in dense plasmas is given, in atomic units, by

$$H_1 = -\frac{1}{2}\sum_{i}^{2}\nabla_i^2 - 2\left[\frac{exp(-\mu r_1)}{r_1} + \frac{exp(-\mu r_2)}{r_2}\right] + \frac{exp(-\mu r_{12})}{r_{12}} \tag{8}$$

where r_1 and r_2 are the radius vectors of the twoelectrons relative to the nucleus, and $r_{12} = |r_1 - r_2|$ is their relative distance.

Moreover, the nonrelativistic Hamiltonian in the effective ECSCP is given by

$$H_2 = -\frac{1}{2}\sum_{i}^{2}\nabla_i^2 - 2\left[\frac{exp(-\mu r_1)}{r_1}\cos(\mu r_1) + \frac{exp(-\mu r_2)}{r_2}\cos(\mu r_2)\right] + \frac{exp(-\mu r_{12})}{r_{12}}\cos(\mu r_{12}) \quad (9)$$

The ground state of the helium atom is a spin singlet two-electron atom. Our calculations for this two-electron system depend on using an ultracompact accurate symmetric function, a nontrivial seven-parameter function, which is constructed by Turbiner et al. [48] as follows:

$$\Psi = (1 + P_{12})[\phi(r_1, r_2)\chi_A] \quad (10)$$

with space wave function:

$$\phi(r_1, r_2) = (1 - ar_1 + br_{12})e^{-\alpha_1 z r_1 - \beta_1 z r_2 + \gamma r_{12}\frac{1+cr_{12}}{1+dr_{12}}} \quad (11)$$

where $a, b, c, d, \alpha_1, \beta_1, \gamma$ are z-dependent parameters and P_{12} is a permutation operator. This function leads for helium atom ($Z = 2$) to a certain improvement of the variational energy and the electron–nuclear cusp and at the same time, the electron–electron cusp. The function χ_A represents the antisymmetric spin wave function with (α) spin up and (β) spin down as follows:

$$\chi_A = \alpha(1)\beta(2) - \alpha(2)\beta(1) \quad (12)$$

This function allows us to obtain the same relative accuracy in both cusp parameters and electronic correlation energy. The function appears as a uniform, locally accurate approximation of the exact ground state eigenfunction. It provides the same relative accuracies in energies and several expectation values together with both cusp parameters.

5. Trial Wave Functions for the Low-Lying Excited States of the Helium Atom

The study of the low-lying excited states of the helium atom has received considerable attention in theoretical investigations. Therefore, for the lowest two excited states, corresponding to the configurations 1s2s, we used the following trial wave functions:

1. For the lowest ortho (space-antisymmetric) state 2^3S, corresponding to the configuration 1s2s, we considered the following simple trial wave function

$$\Psi_{2^3S}(r_1, r_2) = N[(\psi_{1s}(r_1)\psi_{2s}(r_2) - \psi_{1s}(r_2)\psi_{2s}(r_1))\chi_s]f(r_{12}). \quad (13)$$

2. The state 2^1S is a para (space-symmetric) state corresponding to the configuration 1s2s and its trial wave function is, then, taken of the form

$$\Psi_{2^1S}(r_1, r_2) = N[(\psi_{1s}(r_1)\psi_{2s}(r_2) + \psi_{1s}(r_2)\psi_{2s}(r_1))\chi_A]f(r_{12}). \quad (14)$$

In these equations, z_0 and z_i are variational parameters and N is the normalization constant. For spin functions, χ_A represents the singlet antisymmetric spin wave function with (α) spin up and (β) spin down as described in Equation (12).

The function $f(r_{12})$ is the Jastrow correlation function given by [49]

$$f(r_{12}) = e^{\frac{r_{12}}{\alpha_2(1+\beta_2 r_{12})}}, \quad (15)$$

where α_2 and β_2 are variational parameters.

For the relationship of the electron–electron interaction, one obtains the cusp conditions

$$\left.\begin{array}{l} \frac{1}{\Psi}\frac{\partial\Psi}{\partial r_{ij}}\Big|_{r_{ij}=0} = \frac{1}{2} \text{ for unlike spins} \\ \frac{1}{\Psi}\frac{\partial\Psi}{\partial r_{ij}}\Big|_{r_{ij}=0} = \frac{1}{4} \text{ for like spins} \end{array}\right\}.$$

6. Lagrange Mesh Method

The Lagrange mesh method (LMM) [50–52] is a numerical procedure wherein the Schrödinger equation is placed into a nonuniform heterogeneous lattice defined by zeroes of classical orthogonal polynomials, using a basis of Laguerre functions and the associated Gauss quadratures. An exhaustive compilation of accurate energies using the LMM for the He-like atoms can be found in [53]. The wave function is expressed in terms of the perimetric coordinates [54,55]. We employed the lattice parameters [56] $N_x = N_y = 50$, $N_z = 40$, and the scaling parameters $h_x = h_y = 0.3$, $h_z = 0.4$. We used the suitably modified PERILAG code [50] in order to implement the screened Coulomb potentials given by Equations (1), (3) and (5). This code was recently employed [57,58] to carry out accurate calculations of energy for the ground and excited electronic states of He-like atoms embedded inside different plasma model potentials.

7. Results and Discussion

The numerical method used in our calculations, the VMC method, is based on a combination of the well-known variational method and the Monte Carlo technique of calculating the multidimensional integrals. By a suitable choice of the trial wave function, it is then possible to obtain minimum energy eigenvalues in agreement with the exact values for the ground as well as the excited states of the given atom. Accordingly, we investigated the effect of the plasma environment by using the SCP and the ECSCP models on the energy eigenvalues of the helium atom. The calculations are performed using a set of 10^8 Monte Carlo integration points to assess the accuracy with standard deviation of the order 10^{-5}. All our results are obtained in atomic units, i.e., $(\hbar = e = m_e = 1)$. For the value of the ground state energy of the He atom that corresponds to Debye screening length $\lambda_D = \infty$ with screening parameter $\mu = 0.0$ and expresses the case of pure Coulomb potential, we obtained the value -2.902662 a.u., which nearly coincides with the value -2.9027 reported in [48].

Table 1 shows the ground state energies of the helium atom under effective SCP in dense quantum plasma with the He^+ threshold energies and ionization potential $[E_{He^+} - E_{He}]$ of He. The results show good agreement with the most accurate previous results, where the z parameter equals 2, and it is equivalent to the atomic nuclear charge for screening parameter $\mu < 0.5$ ($\lambda_D > 2$, Debye screening length). For $\mu > 0.5$, the parameter z starts to decrease slightly around the value 2; at $\mu = 0.5, z \approx 1.9$ and at $\mu = 1$, $z \approx 1.78$.

In Table 2, we present the ground state energies of the helium atom under effective ECSCP in dense quantum plasma. The He^+ threshold energies and ionization potential $[E_{He^+} - E_{He}]$ of He are also given.

In Table 3, we present the results of our calculations of the ground state energies of the helium atom under Hulthén potential in dense quantum plasma with the He^+ threshold energies and ionization potential $[E_{He^+} - E_{He}]$ of He. For the one electron atoms, the energy ordering of $E^{\mu}_{Hulthen} < E^{\mu}_{SCP} < E^{\mu}_{ECSCP}$, has been a well-known consequence of the comparison theorem [34]. More recently, based on a detailed mathematical analysis, a similar ordering has been conjectured for the He-like atoms [57]. For the ground state He, the proposed conjecture has been validated numerically [25,56]. The energy data presented in Tables 1–3 is employed in Figure 1, where we display the variation of E^{μ}_{SCP}, E^{μ}_{ECSCP}, and $E^{\mu}_{Hulthen}$ as a function of μ. The adherence to the energy ordering $E^{\mu}_{Hulthen} < E^{\mu}_{SCP} < E^{\mu}_{ECSCP}$ is numerically validated for the He atom in its ground state.

Another interesting ordering of energy levels for the one electron atoms is given by $E^{\mu}_{Hulthen} < E^{\mu}_{SCP} < E^{2\mu}_{Hulthen} < E^{\mu}_{ECSCP}$, where $E^{2\mu}_{Hulthen}$ denotes the energy of the Hulthén potential at the screening parameter of 2μ, as defined in Equation (4). As a natural extension of the conjecture [56], this energy ordering is now tested numerically for the He atom in the ground and a few excited states.

Table 1. Ground state energies of the helium atom under effective SCP in dense quantum plasma. The He^+ threshold energies and ionization potential $[E_{He^+} - E_{He}]$ of He are also given.

μ	$-E_{He}$	$-E_{He^+}$	$-[E_{He^+} - E_{He}]$
0	2.902662	2.000000	0.902662
	2.903724^4	2.000000^4	0.903724^4
	2.90337^{16}	-	-
0.01	2.872771	1.980070	0.892701
	2.873839^4	1.980075^4	0.893764^4
0.02	2.843117	1.960268	0.882849
	2.844181^4	1.960298^4	0.883883^4
0.04	2.784473	1.920408	0.864065
0.05	2.755475	1.901848	0.853627
	2.756549^4	1.901845^4	0.854704^4
0.1	2.613758	1.807262	0.806496
	2.614853^4	1.807266^4	0.807587^4
	2.61451^{16}	-	-
0.2	2.345674	1.628183	0.717491
	2.347006^4	1.628232^4	0.718774^4
	2.34666^{16}	-	-
0.4	1.864564	1.306890	0.557674
	1.868451^4	1.307234^4	0.561217^4
0.5	1.652445	1.162981	0.489464
	1.655401^4	1.163678^4	0.491723^4
	1.65504^{16}	-	-
1	0.803519	0.585547	0.217972
	0.818214^4	0.592468^4	0.225746^4
	0.81704^{16}	-	-

Table 2. Ground state energies of the helium atom under effective ECSCP in dense quantum plasma. The He^+ threshold energies and ionization potential $[E_{He^+} - E_{He}]$ of He are also given.

μ	$-E_{He}$	$-E_{He^+}$	$-[E_{He^+} - E_{He}]$
0	2.902662	2.000000	0.902662
	2.903724^5	2.000000^5	0.903724^5
	2.90337^{16}	-	-
0.01	2.872533	1.979987	0.892546
	2.873725^5	1.979988^5	0.893737^5
0.02	2.842163	1.959989	0.882174
	2.843730^5	1.959991^5	0.883739^5
0.04	2.780706	1.919235	0.861471
0.05	2.749620	1.900052	0.849568
	2.753816^5	1.900048^5	0.853768^5
0.1	2.590905	1.800491	0.790414
	2.604436^5	$1.800457^{5]}$	0.803978^5
	2.60409^{16}	-	-
0.2	2.259199	1.603504	0.655695
	2.309111^5	1.603527^5	0.705587^5
0.4	1.770741	1.225043	0.545698
0.5	1.444394	1.046606	0.397788
	1.476958^5	1.047060^5	0.429898^5
	1.47653^{16}	-	-
1	0.402097	0.296429	0.105668
	0.405261^5	0.310714^5	0.094547^5

In Table 4, we list the VMC estimates of $E^{\mu}_{Hulthen}$, E^{μ}_{SCP}, $E^{2\mu}_{Hulthen}$, and E^{μ}_{ECSCP} for $\mu = 0 - 1.0$ corresponding to the ground state He. The LMM estimates are given below the VMC estimates in each case. The two sets of values are found to be in good agreement with each other. The LMC estimates are uniformly below the VMC results. The latter values

can in principle be improved further following a more accurate choice of the trial wave function. In Table 4, we present the results of our calculations of ground state energy for He corresponding to the Hulthen (μ), SCP, Hulthen (2μ), and ECSCP potentials, given by Equations (1), (2), (4) and (5), respectively, over a representative set of μ values. In each case, we include the estimates obtained from the LMM and the VMC calculations. A numerical validation of the energy ordering $E^{\mu}_{Hulthen} < E^{\mu}_{SCP} < E^{2\mu}_{Hulthen} < E^{\mu}_{ECSCP}$ for the ground state He atom is evident from the data in Table 4. It is clear from the present calculations that the inclusion of $E^{2\mu}_{Hulthen}$ makes the bounds to E^{μ}_{SCP} tighter than given by the ordering without $E^{2\mu}_{Hulthen}$.

Table 3. Ground state energies of the helium atom under Hulthén potential in dense quantum plasma. The He^{+} threshold energies and ionization potential $[E_{He^{+}} - E_{He}]$ of He are also given.

μ	$-E_{He}$	$-E_{He^{+}}$	$-[E_{He^{+}} - E_{He}]$
0	2.902662	2.000000	0.902662
0.01	2.887679	1.989821	0.897858
0.02	2.872731	1.979252	0.893479
0.04	2.842973	1.960275	0.882698
0.05	2.828137	1.949522	0.878615
0.1	2.754565	1.900474	0.854091
0.2	2.610298	1.804300	0.805998
0.4	2.333143	1.619535	0.713608
0.5	2.200208	1.530918	0.669290
1	1.592340	1.124164	0.468176

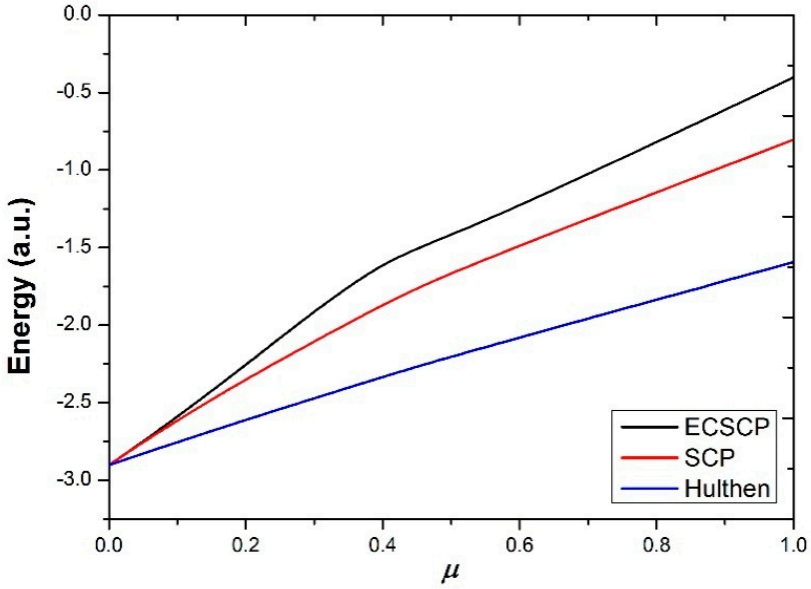

Figure 1. Groundstate energy of the helium atom in SCP, ECSCP, and Hulthén potentials for different values of the screening parameter μ.

In Tables 5 and 6, we present the results of our calculations of $E^{\mu}_{Hulthen}$, E^{μ}_{SCP}, E^{μ}_{ECSCP}, and $E^{2\mu}_{Hulthen}$ corresponding to the (1s2s) excited states of ^1S and ^3S. As observed in the case of the ground state He in Table 4, the VMC and the LMM estimates are in good agreement with each other and the comparison theorembased ordering $E^{\mu}_{Hulthen} < E^{\mu}_{SCP} < E^{2\mu}_{Hulthen} < E^{\mu}_{ECSCP}$ is also obeyed in the excited states. To the best of our knowledge, Tables 4–6 present for the first time numerical validation of the conjecture $E^{\mu}_{Hulthen} < E^{\mu}_{SCP} < E^{2\mu}_{Hulthen} < E^{\mu}_{ECSCP}$ for the ground and excited states of the He atom.

Table 4. Comparison between (a) LMM and (b) VMC for the ground state energies of the helium atom under $E^{\mu}_{Hulthen}$, E^{μ}_{SCP}, $E^{2\mu}_{Hulthen}$, and E^{μ}_{ECSCP}.

μ	Hulthen (μ)	SCP	Hulthén (2μ)	ECSCP
0	−2.903724377 [a] −2.902662 [b]	−2.903724377 [a] −2.902662 [b]		−2.903724377 [a] −2.902662 [b]
0.01	−2.888743509 [a] −2.887679 [b]	−2.873838795 [a] −2.872771 [b]	−2.873800905 [a] −2.872731 [b]	−2.873725125 [a] −2.872533 [b]
0.02	−2.873800905 [a] −2.872731 [b]	−2.844180576 [a] −2.843117 [b]	−2.84403049 [a] −2.842973 [b]	−2.843730329 [a] −2.842163 [b]
0.04	−2.84403049 [a] −2.842973 [b]	−2.785537653 [a] −2.784473 [b]		−2.783771455 [a] −2.780706 [b]
0.05	−2.829202681 [a] −2.828137 [b]	−2.756548811 [a] −2.755475 [b]	−2.755637701 [a] −2.754565 [b]	−2.753815807 [a] −2.749620 [b]
0.1	−2.755637701 [a] −2.754565 [b]	−2.614852947 [a] −2.613758 [b]	−2.611379351 [a] −2.610298 [b]	−2.604435567 [a] −2.590905 [b]
0.2	−2.611379351 [a] −2.610298 [b]	−2.347006184 [a] −2.345674 [b]	−2.334370372 [a] −2.333143 [b]	−2.309114171 [a] −2.259199 [b]
0.4	−2.334370372 [a] −2.333143 [b]	−1.868450546 [a] −1.864564 [b]		−1.742851883 [a] −1.770741 [b]
0.5	−2.201638137 [a] −2.200208 [b]	−1.655401315 [a] −1.652445 [b]	−1.596227498 [a] −1.592340 [b]	−1.47695782 [a] −1.444394 [b]
1	−1.596227498 [a] −1.592340 [b]	−0.818214183 [a] −0.803519 [b]		−0.405261234 [a] −0.402097 [b]

Table 5. Comparison between (a) LMM and (b) VMC for (1s2s) excited states of ^1S energies of the helium atom under $E^{\mu}_{Hulthen}$, E^{μ}_{SCP}, $E^{2\mu}_{Hulthen}$, and E^{μ}_{ECSCP}.

μ	Hulthen (μ)	SCP	Hulthén (2μ)	ECSCP
0	−2.14596983 [a] −2.145788 [b]	−2.14596983 [a] −2.145788 [b]		−2.14596983 [a] −2.145788 [b]
0.01	−2.131029234 [a] −2.129545 [b]	−2.116300015 [a] −2.115372 [b]	−2.116194799 [a] −2.114716 [b]	−2.11598439 [a] −2.113992 [b]
0.02	−2.116194799 [a] −2.114716 [b]	−2.08725862 [a] −2.086387 [b]	−2.086857072 [a] −2.085402 [b]	−2.08605418 [a] −2.085065 [b]
0.03	−2.101470743 [a] −2.100005 [b]	−2.058823511 [a] −2.058013 [b]	−2.05796091 [a] −2.057528 [b]	−2.05623611 [a] −2.055263 [b]
0.04	−2.086857072 [a] −2.085402 [b]	−2.030971244 [a] −2.028217 [b]	−2.029506384 [a] −2.028095 [b]	−2.026576457 [a] −2.025621 [b]
0.05	−2.072353792 [a] −2.070909 [b]	−2.003680728 [a] −2.000982 [b]	−2.001493594 [a] −2.000105 [b]	−1.99711615 [a] −1.994182 [b]
0.06	−2.05796091 [a] −2.056528 [b]	−1.976932817 [a] −1.974287 [b]		−1.967891767 [a] −1.964984 [b]
0.08	−2.029506384 [a] −2.028095 [b]	−1.924996108 [a] −1.922452 [b]		−1.910280654 [a] −1.907431 [b]
0.1	−2.001493594 [a] −2.000105 [b]	−1.875036337 [a] −1.872588 [b]	−1.868060722 [a] −1.866782 [b]	−1.853980921 [a] −1.851209 [b]
0.2	−1.868060722 [a] −1.866782 [b]	−1.651488956 [a] −1.649457 [b]	−1.634414579 [a] −1.633359 [b]	−1.601389925 [a] −1.599132 [b]
0.4	−1.634414579 [a] −1.633359 [b]	−1.304102639 [a] −1.302586 [b]	−1.275179743 [a] −1.274386 [b]	−1.219166537 [a] −1.217393 [b]
0.5	−1.534021688 [a] −1.533064 [b]	−1.158970629 [a] −1.157579 [b]	−1.119597793 [a] −1.118824 [b]	−1.041082207 [a] −1.039325 [b]
0.8	−1.275179743 [a] −1.274386 [b]	−0.787833216 [a] −0.786741 [b]		−0.563849944 [a] −0.562433 [b]
1	−1.119597793 [a] −1.118824 [b]	−0.586621163 [a] −0.585698 [b]		−0.304567693 [a] −0.303396 [b]

Table 6. Comparison between (a) LMM and (b) VMC for (1s2s) excited states of ^3S energies of the helium atom under $E^{\mu}_{Hulthen}$, E^{μ}_{SCP}, $E^{2\mu}_{Hulthen}$, and E^{μ}_{ECSCP}.

μ	Hulthen (μ)	SCP	Hulthén (2μ)	ECSCP
0	−2.175228899 (a) −2.168892 (b)	−2.175228899 (a) −2.168892 (b)		−2.175228899 (a) −2.168892 (b)
0.01	−2.160277331 (a) −2.158999 (b)	−2.145513403 (a) −2.144725 (b)	−2.14542119 (a) −2.143899 (b)	−2.145236778 (a) −2.142392 (b)
0.02	−2.14542119 (a) −2.143899 (b)	−2.11635153 (a) −2.115424 (b)	−2.115996636 (a) −2.114533 (b)	−2.115287001 (a) −2.112255 (b)
0.03	−2.130660957 (a) −2.129201 (b)	−2.08772446 (a) −2.086901 (b)	−2.086955753 (a) −2.085513	−2.085418757 (a) −2.082449 (b)
0.04	−2.115996636 (a) −2.114533 (b)	−2.059614751 (a) −2.058829 (b)	−2.058298598 (a) −2.056876 (b)	−2.05566674 (a) −2.052696 (b)
0.05	−2.101428233 (a) −2.099977 (b)	−2.032006504 (a) −2.029274 (b)	−2.030025255 (a) −2.028622 (b)	−2.026062181 (a) −2.023112 (b)
0.06	−2.086955753 (a) −2.085513 (b)	−2.004885122 (a) −2.002199 (b)		−1.996633374 (a) −1.993701 (b)
0.08	−2.058298598 (a) −2.056876 (b)	−1.952049995 (a) −1.949456 (b)		−1.938404392 (a) −1.935519 (b)
0.1	−2.030025255 (a) −2.028622 (b)	−1.901012328 (a) −1.898506 (b)	−1.894420022 (a) −1.893113 (b)	−1.88116494 (a) −1.878328 (b)
0.2	−1.894420022 (a) −1.893113 (b)	−1.670095721 (a) −1.667977 (b)	−1.652094063 (a) −1.650979 (b)	−1.615667068 (a) −1.613269 (b)
0.4	−1.652094063 (a) −1.650979 (b)	−1.307190384 (a) −1.305633 (b)	−1.276412172 (a) −1.275605 (b)	−1.219400057 (a) −1.217612 (b)
0.5	−1.54542779 (a) −1.544411 (b)	−1.160139744 (a) −1.158742 (b)	−1.120174566 (a) −1.119406 (b)	−1.041273569 (a) −1.039521 (b)
0.8	−1.276412172 (a) −1.275605 (b)	−0.7882615 (a) −0.7871699 (b)		−0.564149249 (a) −0.5627306 (b)
1	−1.120174566 (a) −1.119406 (b)	−0.587027809 (a) −0.5861029 (b)		−0.305119077 (a) −0.3039526 (b)

From the Hamiltonian form of the two-body interactions, the overall potential strength decreases when going from pure Coulomb potentials to SCP and to ECSCP. Physically, we expect for screened potentials that the energy levels increase as μ increases. Furthermore, due to stronger screening effects, for a given μ, the ECSCP values should lie above the corresponding SCP data. Figure 1 represents this situation.

8. Conclusions

In our opinion, the present study is a useful contribution to understanding the ground and a few low-lying excited states of two electron atoms under the influence of three commonly used model potentials describing the plasma environment. The computations are carried out using accurate numerical algorithms based on the VMC and the Lagrange mesh methods. A comprehensive set of numerical results including the ground state of Helium ($1s^2$) is presented, which describe the screening of charges in a plasma where both positive and negative charges are present, and where their motion is thermal. Furthermore, we carried out an investigation to determine the effect of Debye plasma and dense quantum plasmas on the low-lying excited states of helium atom using trial wave functions for the lowest two excited states, corresponding to the configuration 1s2s. The energy ordering of $E^{\mu}_{Hulthen}$, E^{μ}_{SCP}, E^{μ}_{ECSCP}, and $E^{2\mu}_{Hulthen}$ derived from the comparison theorem of quantum mechanics for the hydrogen-like atoms is successfully tested numerically for the He atom in the ground and a few low-lying excited states, which vindicates the proposed conjecture [57] for the first time for the ground as well as the excited states, thus implying the general validity of the comparison theorem in the presence of electron repulsion interaction.

Author Contributions: S.B.D. and K.D.S.: visualization, supervision, investigation, computations, formal analysis, writing—original draft, review and editing, software, visualization, supervision. M.A.S.: writing—review and editing, formal analysis, computations. All authors have read and agreed to the published version of the manuscript.

Funding: This research received no external funding.

Institutional Review Board Statement: Not applicable.

Informed Consent Statement: Not applicable.

Data Availability Statement: No supporting data reported.

Acknowledgments: K.D.S. thanks the Indian National Science Academy, New Delhi, for the award of a senior scientist status. He is also grateful to Daniel Baye for a copy of the PERILAG code. We thank the anonymous reviewers for their helpful suggestions.

Conflicts of Interest: The authors declare no conflict of interest.

References

1. Ghoshal, A.; Ho, Y.K. An Investigation on the $He^-(1s2s^2\,^2S)$ Resonance in Debye Plasmas. *Atoms* **2017**, *5*, 2. [CrossRef]
2. Ning, Y.; Yan, Z.C.; Ho, Y.K. Quantum entanglement for helium atom in the Debye plasmas. *Phys. Plasmas* **2015**, *22*, 013302. [CrossRef]
3. Ning, Y.; Yan, Z.-C.; Ho, Y.K. Natural and Unnatural Parity Resonance States in the Positron-Hydrogen System with Screened Coulomb Interactions. *Atoms* **2015**, *4*, 3. [CrossRef]
4. Kar, S.; Ho, Y.K. Bound states of helium atom in dense plasmas. *Int. J. Quantum Chem.* **2005**, *106*, 814–822. [CrossRef]
5. Ghoshal, A.; Ho, Y.K. Ground states of helium in exponential-cosine-screened Coulomb potentials. *J. Phys. B At. Mol. Opt. Phys.* **2009**, *42*. [CrossRef]
6. Kar, S.; Ho, Y.K.; Jiang, Z. Dispersion coefficients for interactions between hydrogen and helium atoms with Coulomb and screened Coulomb potentials. *J. Phys. B At. Mol. Opt. Phys.* **2011**, *44*. [CrossRef]
7. Kar, S.; Ho, Y. Doubly-excited $2s^{21}$Se resonance state of helium embedded in Debye plasmas. *Chem. Phys. Lett.* **2005**, *402*, 544–548. [CrossRef]
8. Janev, R.; Zhang, S.-B.; Wang, J. Review of quantum collision dynamics in Debye plasmas. *Matter Radiat. Extrem.* **2016**, *1*, 237–248. [CrossRef]
9. Margenau, H.; Lewis, M. Structure of Spectral Lines from Plasmas. *Rev. Mod. Phys.* **1959**, *31*, 569–615. [CrossRef]
10. Shukla, P.; Eliasson, B. Screening and wake potentials of a test charge in quantum plasmas. *Phys. Lett. A* **2008**, *372*, 2897–2899. [CrossRef]
11. Lin, C.Y.; Ho, Y.K. Effects of screened Coulomb (Yukawa) and exponential-cosine-screened Coulomb potentials on photoionization of H and He+. *Eur. Phys. J. D* **2010**, *57*, 21–26. [CrossRef]
12. Soylu, A. Plasma screening effects on the energies of hydrogen atom. *Phys. Plasmas* **2012**, *19*, 072701. [CrossRef]
13. Chang, T.N.; Fang, T.K. Atomic photoionization in a changing plasma environment. *Phys. Rev. A* **2013**, *88*. [CrossRef]
14. Ghoshal, A.; Ho, Y.K. Doubly excited resonance states of helium in exponential cosine-screened Coulomb potentials. *Phys. Rev. A* **2009**, *79*, 062514. [CrossRef]
15. Ghoshal, A.; Ho, Y.K. Properties of hydrogen molecular ion with static screened coulomb and exponential cosine screened coulomb potentials. *Int. J. Quantum Chem.* **2011**, *111*, 4288–4295. [CrossRef]
16. Ancarani, L.U.; Rodriguez, K.V. Correlated expansions of n1S and n3S states for two-electron atoms in exponential cosine screened potentials. *Phys. Rev. A* **2014**, *89*, 012507. [CrossRef]
17. Fang, T.K.; Wu, C.S.; Gao, X.; Chang, T.N. Redshift of the Heα emission line of He-like ions under a plasma environment. *Phys. Rev. A* **2017**, *96*, 052502. [CrossRef]
18. Lin, Y.-C.; Lin, C.-Y.; Ho, Y.K. Spectral/structural data of helium atoms with exponential-cosine-screened coulomb potentials. *Int. J. Quantum Chem.* **2015**, *115*, 830–836. [CrossRef]
19. Roy, A.K. Critical parameters and spherical confinement of H atom in screened Coulomb potential. *Int. J. Quantum Chem.* **2016**, *116*, 953–960. [CrossRef]
20. Ghoshal, A.; Ho, Y.K. Two-Electron System in The Field of Generalized Screened PotentiaL. *Mod. Phys. Lett. B* **2011**, *25*, 1619–1629. [CrossRef]
21. Nasser, I.; Zeama, M.; Abdel-Hady, A. The Rényi entropy, a comparative study for He-like atoms using the exponential-cosine screened Coulomb potential. *Results Phys.* **2017**, *7*, 3892–3900. [CrossRef]
22. Nasyrov, V.V. Radial correlation of the helium atom in the ground state. *J. Exp. Theor. Phys.* **2017**, *125*, 369–371. [CrossRef]
23. Bressanini, D.; Morosi, G. A compact boundary-condition- determined wavefunction for two-electron atomic systems. *J. Phys. B At. Mol. Opt. Phys.* **2008**, *41*. [CrossRef]
24. Rodriguez, K.V.; Gasaneo, G.; Mitnik, D.M. Accurate and simple wavefunctions for the helium isoelectronic sequence with correct cusp conditions. *J. Phys. B At. Mol. Opt. Phys.* **2007**, *40*, 3923–3939. [CrossRef]

25. Zhang, Y.Z.; Jiao, L.G.; Liu, F.; Liu, A.H.; Ho, Y.K. Energy levels of ground and singly excited states of two-electron atoms in dense quantum plasmas. *At. Data Nucl. Data Tables* **2021**, *140*, 101420. [CrossRef]
26. Wang, X.; Jiang, Z.; Kar, S.; Ho, Y.K. The ^{1,3}P0 states of exponential cosine-screened helium like atoms. *At. Data and Nucl. Data Tables* **2021**, in press.
27. Papoulis, A. *Probability, Random Variables, and Stochastic Processes*; McGraw-Hill: New York, NY, USA, 1965.
28. Metropolis, N.; Rosenbluth, A.W.; Rosenbluth, M.N.; Teller, A.H.; Teller, E. Equation of State Calculations by Fast Computing Machines. *J. Chem. Phys.* **1953**, *21*, 1087–1092. [CrossRef]
29. Doma, S.B.; Abu-Shady, M.; El-Gammal, F.N.; Amer, A.A. Ground states of the hydrogen molecule and its molecular ion in the presence of a magnetic field using the variational Monte Carlo method. *Mol. Phys.* **2016**, *114*, 1787–1793. [CrossRef]
30. Doma, S.; Shaker, M.O.; Farag, A.M.; El-Gammal, F. Ground States of Helium Atom and Hydrogen Negative Ion in the Presence of Magnetic Field Using Variational Monte Carlo Technique. *Acta Phys. Pol. A* **2014**, *126*, 700–705. [CrossRef]
31. Doma, S.B.; Shaker, M.O.; Farag, A.M.; El-Gammal, F.N. Variational Monte Carlo calculations of lithium atom in strong magnetic field. *J. Exp. Theor. Phys.* **2017**, *124*, 1–9. [CrossRef]
32. Baye, D. The Lagrange-mesh method. *Phys. Rep.* **2014**, *565*, 1–107. [CrossRef]
33. Thirring, W. *A Course in Mathematical Physics 3: Quantum Mechanics of Atoms and Molecules*; Springer: New York, NY, USA, 1981.
34. Wang, X.R. General theorem on the Schrödinger equation. *Phys. Rev. A* **1992**, *46*, 7295–7296. [CrossRef] [PubMed]
35. Hall, R. Refining the comparison theorem of quantum mechanics. *J. Phys. A Math. Gen.* **1992**, *25*, 4459–4469. [CrossRef]
36. Santos, E.S.; Rivelino, R.; De Montigny, M.; De Melo, G.R. A spin Hamiltonian for non-relativistic electrons and their interaction with an external field. *J. Phys. A Math. Theor.* **2010**, *43*. [CrossRef]
37. Ragusa, M.A.; Tachikawa, A. On continuity of minimizers for certain quadratic growth functionals. *J. Math. Soc. Jpn.* **2005**, *57*. [CrossRef]
38. Fassari, S. On the bound states of non-relativistic Krönig-Penney Hamiltonians with short range impurities. *Helv. Phys. Acta* **1990**, *63*, 849–883.
39. Hall, R.L.; Katatbeh, Q.D. Generalized comparison theorems in quantum mechanics. *J. Phys. A Math. Gen.* **2002**, *35*, 8727–8742. [CrossRef]
40. Chen, G. Spectral comparison theorem for theN-dimensional Dirac equation. *Phys. Rev. A* **2005**, *72*, 044102. [CrossRef]
41. Hall, R.L. Special Comparison Theorem for the Dirac Equation. *Phys. Rev. Lett.* **2008**, *101*, 090401. [CrossRef] [PubMed]
42. Hall, R.L.; Yeşiltaş, Ö. Comparison theorems for the Dirac equation with spin-symmetric and pseudo-spin-symmetric interactions. *J. Phys. A Math. Theor.* **2010**, *43*. [CrossRef]
43. Semay, C. General comparison theorem for eigenvalues of a certain class of Hamiltonians. *Phys. Rev. A* **2011**, *83*. [CrossRef]
44. Ichimaru, S.; Iyetomi, H.; Tanaka, S. Statistical physics of dense plasmas: Thermodynamics, transport coefficients and dynamic correlations. *Phys. Rep.* **1987**, *149*, 91–205. [CrossRef]
45. Hulthén, L. On the characteristic solutions of the Schrödinger deuteron equation. *Ark. Met. Astron. Fys. A* **1942**, *28*, 5.
46. Pottorf, S.; Pudzerd, A.; Choud, M.Y.; Hasbun, J.E. The simple harmonic oscillator ground state using a variational Monte Carlo method. *Eur. J. Phys.* **1999**, *20*, 205–212. [CrossRef]
47. Ruiz, M.B. Hylleraas method for many-electron atoms. I. The Hamiltonian. *Int. J. Quantum Chem.* **2004**, *101*, 246–260. [CrossRef]
48. Turbiner, A.V.; del Valle, J.C.; Vieyra, J.C.L.; Nader, D.J. Ultra-compact accurate wave functions for He-like and Li-like iso-electronic sequences and variational calculus: I. Ground state. *Int. J. Quantum Chem.* **2021**, *121*, e26586. [CrossRef]
49. Filippi, C.; Umrigar, C.J. Multiconfiguration wave functions for quantum Monte Carlo calculations of first-row diatomic molecules. *J. Chem. Phys.* **1996**, *105*, 213–226. [CrossRef]
50. Hesse, M.; Baye, D. Lagrange-mesh calculations of three-body atoms and molecules. *J. Phys. B At. Mol. Opt. Phys.* **1999**, *32*, 5605–5617. [CrossRef]
51. Baye, D.; Sen, K.D. Confined hydrogen atom by the Lagrange-mesh method: Energies, mean radii, and dynamic polarizabilities. *Phys. Rev. E* **2008**, *78*, 026701. [CrossRef]
52. Montgomery, J.H.E.; Sen, K.D.; Katriel, J. Critical screening in the one- and two-electron Yukawa atoms. *Phys. Rev. A* **2018**, *97*, 022503. [CrossRef]
53. Turbiner, A.V.; Vieyra, J.C.L.; Olivares-Pilón, H. Few-electron atomic ions in non-relativistic QED: The ground state. *Ann. Phys.* **2019**, *409*, 167908. [CrossRef]
54. Coolidge, A.S.; James, H.M. On the Convergence of the Hylleraas Variational Method. *Phys. Rev.* **1937**, *51*, 855–859. [CrossRef]
55. Pekeris, C.L. Ground State of Two-Electron Atoms. *Phys. Rev.* **1958**, *112*, 1649–1658. [CrossRef]
56. Bollhöfer, M.; Notay, Y. JADAMILU: A software code for computing selected eigenvalues of large sparse symmetric matrices. *Comput. Phys. Commun.* **2007**, *177*, 951–964. [CrossRef]
57. Sen, K.; Katrielb, J.; Montgomery, H. A comparative study of two-electron systems with screened Coulomb potentials. *Ann. Phys.* **2018**, *397*, 192–212. [CrossRef]
58. Adan, M.; Sanchez, M.; Martinez-Flores, C.; Vargas, R.; Cabera-Trujillo, R.; Garza, J.; Sen, K.D. Ionization of many-electron atoms by the action of two plasma models. *Phys. Rev. E* **2021**, *103*, 043202.